Eur. J. Mech. B/Fluids, **18**, n° 2, 227-243, 1999

Interactions between pairs of oblique waves in a Bickley jet

R. MALLIER *, M. HASLAM

ABSTRACT. – We consider the weakly nonlinear spatial evolution of a pair of varicose oblique waves and a pair of sinuous oblique waves superimposed on an inviscid Bickley jet, with each wave being slightly amplified on a linear basis. The two pairs are assumed to both be inclined at the same angle to the plane of the jet. A nonlinear critical layer analysis is employed to derive equations governing the evolution of the instability wave amplitudes, which contain a coupling between the modes. These equations are discussed and solved numerically, and it is shown that, as in related work for other flows, these equations may develop a singularity at a finite distance downstream.© Elsevier, Paris.

1. Introduction

In a landmark paper, Goldstein and Choi (1989) identified a critical layer mechanism by which oblique disturbances to a shear layer could undergo extremely rapid growth when the disturbance consisted of a pair of oblique waves at equal and opposite angles to the shear layer. This mechanism was similar to that for a single wave found earlier by Hickernell (1984), and the amplitude equations arising from the theory of nonlinear non-equilibrium critical layers are sometimes called "Hickernell-type" equations. Later (Goldstein and Lee, 1992; Wu, 1992), it was found that the growth could be even more rapid if in addition to the pair of oblique waves, the disturbance included a plane wave. This approach required that the oblique waves be the subharmonic of the plane wave, meaning that they had to be inclined at $\pm 60^\circ$ to the plane of the mean flow, and this form of disturbance is known as a (subharmonic) resonant triad. If the amplitude of the disturbance was $\mathcal{O}(\varepsilon)$, the evolution of a purely planar disturbance would first become nonlinear on a length-scale (or time-scale for temporally evolving disturbances) of $\mathcal{O}(\varepsilon^{-1/2})$ while a disturbance consisting of a pair of oblique waves would first experience nonlinear growth on the much shorter length-scale of $\mathcal{O}(\varepsilon^{-1/3})$ and the length-scale for a resonant triad was $\mathcal{O}(\varepsilon^{-1/4})$ for the parametric resonance stage. In all cases, the growth first became nonlinear inside the critical layer, which is the location at which the velocity of the base flow is equal to the phase speed of the disturbance, $u_0(y_c) = c$. Mathematically, the approach taken in these studies was to employ matched asymptotic expansions, with an "outer" expansion away from the critical layer and an "inner" expansion near the critical layer, where rescaled variables were introduced.

A number of studies followed for various flows (e.g. Goldstein, 1994; Wu, Lee and Cowley, 1993; Mallier and Maslowe, 1994a, 1994b), and it has been claimed (e.g. Mallier and Maslowe, 1994b) that some experiments (e.g. Corke and Kusek, 1993) have provided at least partial confirmation of the theory. Most of the studies cited above considered flows with only one critical layer, although Wu's (1992) study of the Stokes layer allowed the possibility of more than one critical layer but did not explore possible interactions between different

* Correspondence and reprints.
Department of Applied Mathematics, The University of Western Ontario, London ON N6A 5B7, Canada.

0997-7546/99/02/© Elsevier, Paris

neutral modes. For plane wakes and jets, it is well known that there may be two different types of neutral modes with critical layers centered on the inflection points, viz. the sinuous and varicose modes. The Bickley jet is somewhat special in that the neutral varicose mode is the subharmonic of the neutral sinuous mode, and several studies have explored the possibility of an interaction between these two modes. Wygnanski *et al.* (1986) conducted careful experiments on small deficit (turbulent) wakes and found that the development of some aspects of the flow was dependent on initial conditions, which they attributed to interactions between the varicose and sinuous modes, and other experiments (e.g. Sato, 1970; Sato and Saito, 1978) have also suggested that these interactions may take place. One reason why it was thought that such interactions might be important was that they could cause the nonlinear growth of disturbances to be even more rapid than that attributable to the resonance mechanisms discussed above. Very rapid amplification of three-dimensional disturbances has indeed been observed in plane wakes in both experiments (e.g. Corke *et al.*, 1992; Williamson and Prasad, 1993a,b), and numerical simulations (Sondergaard *et al.*, 1994, 1997).

Kelly (1968) used Stuart-Watson type nonlinear stability theory to investigate interactions of the form discussed above; however, he found that there was no modal interaction of the type assumed. Later, Leib and Goldstein (1989) re-examined the problem for purely two-dimensional disturbances using a nonlinear-nonequilibrium critical layer, and they found that there was indeed an interaction between the modes. Mallier (1996), studied the possibility of an interaction between a pair of resonant triads in the Bickley jet, with one triad consisting of a plane sinuous mode together with a pair of oblique sinuous modes inclined at $\pm 60^{\circ}$ and the other triad consisting of a plane varicose mode together with a pair of oblique varicose modes also inclined at $\pm 60^{\circ}$, and again it was found that interactions could occur. The study by Mallier essentially covered three stages: a linear stage when the amplitudes of the disturbances were very small, the "parametric resonance" stage, and the so-called "fully-coupled" stage. The amplitude equations presented were of course for the third (fully-coupled) stage, but the two earlier stages could be recovered from these equations by rescaling the amplitudes, as discussed in Goldstein & Lee (1992). The study of the fully-coupled stage was a little restrictive in that it was necessary to assume that, in that stage, the varicose oblique modes were larger than any of the other waves present which is at odds with the linear theory which says that the linear growth rates of the sinuous modes are larger than those of the varicose modes. This was because in the earlier parametric resonance stage, when it was assumed that all of the waves were of the same order of magnitude, it had been found that the varicose oblique waves underwent very rapid growth while the plane waves and the sinuous oblique waves continued to grow exponentially in a linear fashion. The amplitude equations derived in Mallier (1996) are reproduced here in Appendix B. The coupling in these equations was a little unusual in that the sinuous triad did not affect the varicose triad, and therefore equations for the varicose triad were simply those for a single resonant triad (Goldstein and Lee, 1992; Wu, 1992). However, the sinuous triad was strongly affected by presence of the varicose triad, and furthermore, if the varicose triad was absent the nonlinear terms in the equations for the sinuous triad vanished, leaving only linear equations for those modes.

Wu (1996) criticized the study by Mallier on the grounds that in the fully-coupled stage it was assumed that the varicose oblique waves were larger than the other waves, suggesting that some sort of preferential forcing might have to be used in order for such a state to arise, and proposed an alternative mechanism for interactions between the modes, involving what he termed a "phase-locked" interaction (Wu and Stewart, 1996). Wu claimed that this was a more viable mechanism for free transition. However, if we denote (α, β, c) to be the plane and transverse wave numbers and the phase speed respectively, Wu's study involved the modes $(2, 0, c)$, $(7/4, \pm\sqrt{15}/4, c)$ and $(1/4, \pm\sqrt{15}/4, c)$, representing a planar sinuous mode and oblique sinuous and varicose modes respectively. Although this phase-locked interaction is undoubtedly a powerful mechanism, it would seem to require that the oblique sinuous waves and the oblique varicose waves be inclined at angles of about $\pm 29^{\circ}$ and $\pm 76^{\circ}$ respectively, which would also appear to be a somewhat restrictive assumption, although in practice

a small amount of detuning would be allowed. Again, some sort of preferential forcing would presumably need to be present to give rise to this scenario.

In the present study, we point out that there exists a much simpler mechanism than that proposed by either Mallier or Wu, although the mechanisms presented in those studies will of course arise under the appropriate circumstances. The disturbance studied here consists of a pair of oblique sinuous modes together with a pair of oblique varicose modes, with both pairs inclined at the same angle to the plane. Each of these waves is assumed to have an amplitude $\mathcal{O}(\varepsilon)$. The wave numbers and phase speeds of the modes are $(\cos\theta, \pm\sin\theta, 2/3 - \varepsilon^{1/3}c_1)$ for the varicose modes and $(2\cos\theta, \pm 2\sin\theta, 2/3 - \varepsilon^{1/3}c_1)$ for the sinuous modes, where ε is a non-dimensional parameter characterizing the amplitude of the disturbance and θ is the angle that the oblique waves make with the plane. The $\mathcal{O}(\varepsilon^{1/3})$ departure of the phase speed from its neutral value gives rise to a long length-scale $X = \varepsilon^{1/3}x$ on which the waves interact. In the present study, which uses an $\varepsilon^{1/3}$ critical layer similar to that used by Goldstein and Choi (1989), the varicose and oblique waves may be of roughly the same size ($\mathcal{O}(\varepsilon)$) or either of them may be smaller than this, or indeed, one or other of them may be absent altogether in which case the amplitude equation for the remaining pair of waves simply reduces to that of Goldstein and Choi. One possibility allowed by this scaling then is that the sinuous waves be much larger than the varicose modes, in accordance with linear theory, which will still lead to very rapid growth of both the sinuous and varicose waves during this stage.

The structure of the remainder of the paper is as follows. In Section 2, we briefly sketch the flow in the outer region, posing a perturbation analysis outside the critical layer. Since the analysis so closely follows that of the pairs of resonant triads (Mallier, 1996), the procedure will be only briefly sketched. We should note here that, just as in Mallier (1996), it is necessary to include in our analysis a mean streamwise vortex motion both inside and outside the critical layer. Outside the critical layer, the x component of the velocity due to this streamwise vortex is as large ($\mathcal{O}(\varepsilon)$) as the oblique waves which induce it, although the y and z components are smaller. The need for this streamwise vortex was first noted by Goldstein and Choi (1989), and indeed all the scales used in this paper follow exactly those of Goldstein & Choi.

In Section 3, we sketch how to analyze the flow inside the critical layers, again omitting the details because of the similarity to Mallier (1996), and arrive at the relevant jumps across the critical layers, which we match to the jumps from the outer expansion given in Section 2. This leads us to the amplitude equations, which are a pair of coupled nonlinear integro-differential equations governing the amplitudes of the waves. As noted above, when one or other of the pairs of waves is absent, the equation for the remaining pair reduces to that of Goldstein and Choi (1989). As now appears usual for equations of this type, these equations may develop a singularity at a finite distance downstream, the physical significance of which is still not completely understood. To elucidate this behaviour, the amplitude equations are solved numerically, and we find that the location of the downstream singularity is strongly dependent on the angle θ and the initial amplitudes of the waves. Finally, in Section 5, we make some concluding remarks.

2. Formulation and outer expansion

In what follows, since the development so closely mirrors that of Mallier (1996) for the pair of resonant triads, the details will be largely omitted. We consider the spatial stability of the Bickley jet

$$\overline{u}(y) = \operatorname{sech}^2 y \tag{2.1}$$

to perturbations of $\mathcal{O}(\varepsilon)$ where $\varepsilon \ll 1$ is a dimensionless amplitude parameter. For oblique perturbations proportional to $\exp(\imath\alpha(\tilde{x}\cos\theta \pm z\sin\theta))$, where $\tilde{x} = x - ct$, the Bickley jet has two modes with a phase speed

of 2/3 which are neutrally stable on a linear basis, viz. a varicose (odd) mode for which $\alpha = 1$ and a sinuous (even) mode for which $\alpha = 2$. The Bickley jet has 2 critical layers for this phase speed, located at $y = \pm y_c$ where $y_c = \operatorname{arctanh} 3^{-1/2}$, the inflection points of the flow.

The initial perturbation consists of two pairs of oblique waves, with one pair being associated with either of the neutral modes mentioned above, and it is assumed that each pair makes the same angle θ with the plane of the jet. Assuming the flow to be inviscid (which requires in practice that the Reynolds number $\mathrm{Re} \gg \varepsilon^{-1}$) and incompressible, the equations of motion can be written in non-dimensional form as

$$\frac{\partial \underline{q}}{\partial t} + (\underline{q} \bullet \nabla)\underline{q} = -\nabla p \qquad \nabla \bullet \underline{q} = 0, \tag{2.2}$$

where the velocity components $\underline{q} = (\overline{u} + \varepsilon\tilde{u}, \varepsilon\tilde{v}, \varepsilon\tilde{w})$ and the perturbation pressure $p = \varepsilon\tilde{p}$ are expanded as $\tilde{u} = u^{(1)} + \varepsilon^{1/3}u^{(2)} + \varepsilon^{2/3}u^{(3)} + \cdots$ with similar expressions for $\tilde{v}$, $\tilde{w}$ and $\tilde{p}$. The basic pressure is a constant which can be set to zero without any loss of generality. Weak viscosity could be added to this analysis by writing $\mathrm{Re}^{-1} = \varepsilon\lambda$ where λ is the Benney-Bergeron parameter. The lowest order disturbance is composed of a pair of oblique waves of equal amplitude at equal and opposite angles to the mean flow and a varicose disturbance of similar form. The vertical velocity at lowest order can be written as

$$\begin{aligned} v^{(1)} = {} & 2\Big(A_1(X)e^{\imath\alpha\tilde{x}\cos\theta} + A_1^* e^{-\imath\alpha\tilde{x}\cos\theta}\Big)\hat{v}_{11}^{(1)}(y)\cos(\alpha z\sin\theta) \\ & + 2\Big(A_2(X)e^{2\imath\alpha\tilde{x}\cos\theta} + A_2^* e^{-2\imath\alpha\tilde{x}\cos\theta}\Big)\hat{v}_{22}^{(1)}(y)\cos(2\alpha z\sin\theta), \end{aligned} \tag{2.3}$$

where $X = \varepsilon^{1/3}x$ is a long length-scale, $*$ means complex conjugate and $\alpha = 1$ and $c = 2/3 - \varepsilon^{1/3}c_1$. Clearly, $\hat{v}_{11}^{(1)}$ and $\hat{v}_{22}^{(1)}$ are solutions of the Rayleigh equation

$$\hat{v}_{yy} + \left(6\operatorname{sech}^2 y - \alpha^2\right)\hat{v} = 0 \tag{2.4}$$

which vanish as $y \to \pm\infty$. The velocity and pressure components at this order are

$$\begin{aligned} \hat{u}_{11}^{(1)} &= \imath\cos\theta\operatorname{sech} y\left(2\operatorname{sech}^2 y - 1\right) + \frac{6\imath\sin\theta\tan\theta\operatorname{sech}^3 y\tanh^2 y}{2 - 3\operatorname{sech}^2 y} \\ \hat{v}_{11}^{(1)} &= \operatorname{sech} y\tanh y \\ \hat{w}_{11}^{(1)} &= -\frac{\imath\sin\theta\operatorname{sech} y\left(2 - \operatorname{sech}^2 y\right)}{2 - 3\operatorname{sech}^2 y} \\ \hat{p}_{11}^{(1)} &= -\frac{\imath}{3}\cos\theta\operatorname{sech} y\left(2 - \operatorname{sech}^2 y\right) \\ \hat{u}_{22}^{(1)} &= -\imath\cos\theta\operatorname{sech}^2 y\tanh y + \frac{3\imath\sin\theta\tan\theta\operatorname{sech}^4 y\tanh y}{2 - 3\operatorname{sech}^2 y} \\ \hat{v}_{22}^{(1)} &= \operatorname{sech}^2 y \\ \hat{w}_{22}^{(1)} &= -\frac{2\imath\sin\theta\operatorname{sech}^2 y\tanh y}{2 - 3\operatorname{sech}^2 y} \\ \hat{p}_{22}^{(1)} &= -\frac{2\imath}{3}\cos\theta\operatorname{sech} y\tanh y. \end{aligned} \tag{2.5}$$

The $\mathcal{O}(\varepsilon)$ streamwise velocity will also include a spanwise mean flow component induced by the flow inside the critical layer. This was first pointed out by Goldstein and Choi (1989) for a similar problem.

The expansion at higher orders proceeds in a very similar manner to Mallier (1996), and we find that the $\mathcal{O}\left(\varepsilon^{4/3}\right)$ vertical velocity $\hat{v}^{(2)}$ for each of the oblique waves obeys the following equation

$$\mathcal{L}\hat{v}^{(2)} = \left(\frac{18c_1 A}{2\cosh^2 y - 3} + \frac{2\imath\left(6 + 3\alpha^2\cos^2\theta - 2\alpha^2\cos^2\theta\cosh^2 y\right)A'}{\cos\theta\left(2\cosh^2 y - 3\right)}\right)\hat{v}^{(1)}, \tag{2.6}$$

where the left hand side is the Rayleigh operator from (2.4) and of course for the varicose mode A will be replaced by A_1 and $\alpha = 1$ while for the sinuous mode A will be replaced by A_2 and $\alpha = 2$, and $\hat{v}^{(1)}$ are the appropriate solutions from the first order in the expansion. These equations have solutions of the form

$$\hat{v}_{11}^{(2)} = C_{11(\pm)}^{(\pm)}(X)\hat{v}_{11}^{(1)} + D_{11(\pm)}^{(\pm)}(X)\hat{v}_{11}^{(2c)} + \hat{v}_{11}^{(2p)}, \tag{2.7}$$

with $\hat{v}_{22}^{(2)}$ taking a similar form but with the '11's replaced by '22's. The superscripts $(\pm)$ on the D_{mn} and C_{mn} refer to the upper and lower critical layers respectively and the subscripts $(\pm)$ refer to the regions above and below those critical layers. Here, $\hat{v}_{11}^{(2p)}$ is a particular solution to (2.6) and $\hat{v}_{11}^{(2c)}$ is a second linearly independent solution to the Rayleigh equation given by

$$\hat{v}_{11}^{(2c)} = \hat{v}_{11}^{(1)}\int\frac{dy}{\hat{v}_{11}^{(1)2}}. \tag{2.8}$$

We will find expressions for these C_{mn} and D_{mn} from both the outer expansion and the critical layer, and matching these expressions together will yield the amplitude equations. Imposing the condition that the vertical velocities at this order and their first derivatives with respect to y are continuous at the center-line $y = 0$ tells us that $C_{11(+)}^{(-)} = C_{11(-)}^{(+)}$, $C_{22(+)}^{(-)} = C_{22(-)}^{(+)}$, $D_{11(+)}^{(-)} = D_{11(-)}^{(+)}$ and $D_{22(+)}^{(-)} = D_{22(-)}^{(+)}$. We note that although $\hat{v}_{11}^{(1)}$ satisfies the boundary conditions as $y \to \pm\infty$, neither $\hat{v}_{11}^{(2c)}$ nor $\hat{v}_{11}^{(2p)}$ vanish as $y \to \pm\infty$, but $\hat{v}_{11}^{(2)}$ must. Imposing the homogeneous boundary condition on $\hat{v}_{11}^{(2)}$ at $y = \infty$ leads to an expression for $D_{11(+)}^{(+)}$ in terms A_1 and A_1', and similarly we get an expression at $y = -\infty$ for $D_{11(-)}^{(-)}$. Subtracting these two expressions tells us that

$$D_{11(+)}^{(+)} - D_{11(-)}^{(-)} = \imath A_1'\left(\frac{32y_c}{3\sqrt{3}\cos\theta} - \frac{8}{3\cos\theta} + \frac{4\cos\theta}{3}\right) + 4c_1 A_1\left(\frac{2y_c}{\sqrt{3}} - 1\right), \tag{2.9}$$

and similarly we obtain

$$D_{22(+)}^{(+)} - D_{22(-)}^{(-)} = 16\imath A_2'\left(\frac{1}{3\cos\theta} + \frac{\cos\theta}{3} + \frac{y_c}{3\sqrt{3}\cos\theta}\right) - 16c_1 A_2\left(1 + \frac{y_c}{\sqrt{3}}\right). \tag{2.10}$$

In the above analysis, it is assumed that $\sin\theta$ and $\cos\theta$ are both $\mathcal{O}(1)$. In the limit $\cos\theta \to 0$, the terms in (2.9), (2.10) involving $1/\cos\theta$ blow up, and this is because in this limit, the disturbance is essentially comprised of a spanwise wave rather than oblique waves, and for this case, which is not covered by the present study, the jump would come in at leading order, $\mathcal{O}(\varepsilon)$, rather than at $\mathcal{O}\left(\varepsilon^{4/3}\right)$. This limit might better be tackled by formally considering a spanwise wave whose amplitude is weakly modulated in the streamwise direction via the long length-scale X, and likewise the limit $\sin\theta \to 0$ might better be tackled by considering a plane wave whose amplitude is weakly modulated in the z-direction via a spanwise long length-scale.

In the next section, we will sketch how to find expressions for these jumps from the critical layer solution; matching these jumps will lead to the amplitude equations governing the spatial evolution of A_1 and A_2.

3. Critical layer analysis

In order to obtain evolution equations for A_1 and A_2, we shall now pose inner expansions in each of the upper and lower critical layers, where the outer expansion becomes disordered, and obtain expressions for the jumps across the critical layers. The details will again be largely omitted, because the analysis so closely parallels that of Mallier (1996), and we will also only consider the upper critical layer because the analysis follows a similar path for both critical layers.

Near the upper critical layer at $y = y_c$, we introduce the rescaled inner variables $Y = \varepsilon^{-1/3}(y - y_c)$, $U = \varepsilon^{-1/3}(u - 2/3)$, $V = \varepsilon^{-2/3}v$, $W = \varepsilon^{-1/3}w$ and $P = \varepsilon^{-4/3}p$, where of course ε was the order of magnitude of the disturbance in the outer expansion and $X = \varepsilon^{1/3}x$ was the long length scale. With these scalings, the governing equations become

$$
\begin{aligned}
\frac{2}{3}U_X + c_1 U_{\tilde{x}} + UU_{\tilde{x}} + \varepsilon^{1/3}U_X + VU_Y + WU_z + \varepsilon^{2/3}P_{\tilde{x}} + \varepsilon P_X &= 0 \\
\frac{2}{3}V_X + c_1 V_{\tilde{x}} + UV_{\tilde{x}} + \varepsilon^{1/3}UV_X + VV_Y + WV_z + P_Y &= 0 \\
\frac{2}{3}W_X + c_1 W_{\tilde{x}} + UW_{\tilde{x}} + \varepsilon^{1/3}UW_X + VW_Y + WW_z + \varepsilon^{2/3}P_z &= 0 \\
U_{\tilde{x}} + \varepsilon^{1/3}U_X + V_Y + W_z &= 0.
\end{aligned}
\tag{3.1}
$$

The form of the inner expansion can be deduced from the solution written in inner variables,

$$
\begin{aligned}
U &= -\frac{4Y}{3^{3/2}} + \varepsilon^{1/3}U_1 + \varepsilon^{2/3}U_2 + \cdots \\
V &= \varepsilon^{1/3}V_1 + \varepsilon^{2/3}V_2 + \cdots \\
W &= \varepsilon^{1/3}W_1 + \varepsilon^{2/3}W_2 + \cdots \\
P &= \varepsilon^{-1/3}P_{-1} + P_0 + \varepsilon^{1/3}P_1 + \varepsilon^{2/3}P_2 + \cdots
\end{aligned}
\tag{3.2}
$$

The streamwise velocity at lowest order can be written as

$$
U_1 = 2\left(U_{11}^{(1)}e^{\imath\alpha\tilde{x}\cos\theta} + c.c.\right)\cos(\alpha z\sin\theta) + 2\left(U_{22}^{(1)}e^{2\imath\alpha\tilde{x}\cos\theta} + c.c.\right)\cos(2\alpha z\sin\theta) \tag{3.3}
$$

where the oblique varicose and sinuous components are respectively

$$
\begin{aligned}
U_{11}^{(1)} &= \frac{2^{3/2}\sin^2\theta}{3^{3/2}}\int_{-\infty}^{X} A_1(X_0)e^{-2\imath\cos\theta\tilde{Y}(X_0-X)/\sqrt{3}}dX_0 \\
U_{22}^{(1)} &= \frac{2^{3/2}\sin^2\theta}{3^{3/2}}\int_{-\infty}^{X} A_2(X_0)e^{-4\imath\cos\theta\tilde{Y}(X_0-X)/\sqrt{3}}dX_0,
\end{aligned}
\tag{3.4}
$$

where $\tilde{Y} = Y - 3^{3/2}c_1/4$. Similarly, for the other velocity and pressure components we find

$$
\begin{aligned}
V_{11}^{(1)} &= \frac{\sqrt{2}}{3}A_1 \\
V_{22}^{(1)} &= \frac{2}{3}A_2 \\
W_{11}^{(1)} &= -\cot\theta U_{11}^{(1)}
\end{aligned}
\tag{3.5}
$$

$$W_{22}^{(1)} = -\cot\theta U_{22}^{(1)}$$
$$P_{11}^{(-1)} = -\imath\frac{2^{5/2}}{3^{5/2}}\cos\theta A_1$$
$$P_{22}^{(-1)} = -\imath\frac{4}{3^{5/2}}\cos\theta A_2$$

Here $U_{mn}^{(l)}$ denotes the term at $\mathcal{O}\left(\varepsilon^{l/3}\right)$ multiplying $\exp\left(i\alpha(m\tilde{x}\cos\theta + nz\sin\theta)\right)$.

As in Mallier (1996), if we consider the pressure at the next order, the outer expansion written in the inner variables involves the functions C_{mn} and D_{mn} which entered into the outer expansion at $\mathcal{O}\left(\varepsilon^{4/3}\right)$. Since the pressure at this order must be continuous at $Y = 0$, this yields the following relations between the C_{mn} and D_{mn},

$$\begin{aligned} C_{11(+)}^{(+)} + 3D_{11(+)}^{(+)}\left(2y_c - \sqrt{3}\right)/4 &= C_{11(+)}^{(-)} + 3D_{11(+)}^{(-)}\left(2y_c - \sqrt{3}\right)/4 \\ C_{22(+)}^{(+)} + 3D_{22(+)}^{(+)}\left(\sqrt{3} + y_c\right)/8 &= C_{22(+)}^{(-)} + 3D_{22(+)}^{(-)}\left(\sqrt{3} + y_c\right)/8 \end{aligned} \tag{3.6}$$

If we proceed with the expansion in a similar manner to Mallier (1996), we find that there are jumps across the critical layer in the derivative of the vertical velocity at $\mathcal{O}(\varepsilon)$ for both the sinuous and varicose oblique modes. These jumps are as follows:

$$\begin{aligned} D_{11(+)}^{(+)} - D_{11(-)}^{(-)} &= \frac{\sqrt{2}}{3}\int_{-\infty}^{\infty}\left(V_{11YY}^{(4)} + \sqrt{2}A_1\right)dY \\ &= \frac{2\imath\pi c_1 A_1}{\sqrt{3}} + \frac{4\pi A_1'}{3\sqrt{3}\cos\theta} \\ &\quad + k_1\int_0^\infty\int_0^\infty \mathcal{R}_1^{(a)}A_1^*(X - 2\tau_0 - \tau_1)A_1(X - \tau_0 - \tau_1)A_1(X - \tau_0)d\tau_0 d\tau_1 \\ &\quad + \int_0^\infty\int_0^\infty \mathcal{R}_1^{(b)}A_2^*(X - 3\tau_0 - \tau_1)A_2(X - 2\tau_0 - \tau_1)A_1(X - 2\tau_0)d\tau_0 d\tau_1 \\ &\quad + \int_0^\infty\int_0^\infty \mathcal{R}_1^{(c)}A_2^*(X - 2\tau_0 - \tau_1)A_2(X - \tau_0)A_1(X - 2\tau_0 - 2\tau_1)d\tau_0 d\tau_1 \\ &\quad + \int_0^\infty\int_0^\infty \mathcal{R}_1^{(d)}A_2^*(X - 3\tau_0 - 2\tau_1)A_2(X - \tau_1 - 2\tau_0)A_1(X - 2\tau_0 - 2\tau_1)d\tau_0 d\tau_1 \end{aligned}$$

$$\begin{aligned} D_{22(+)}^{(+)} - D_{22(-)}^{(-)} &= \frac{2}{3}\int_{-\infty}^{\infty} V_{22YY}^{(4)}dY \\ &= \frac{4\imath\pi c_1 A_2}{\sqrt{3}} + \frac{4\pi A_2'}{3\sqrt{3}\cos\theta} \\ &\quad + k_2\int_0^\infty\int_0^\infty \mathcal{R}_1^{(a)}A_2^*(X - 2\tau_0 - \tau_1)A_2(X - \tau_0 - \tau_1)A_2(X - \tau_0)d\tau_0 d\tau_1 \\ &\quad + \int_0^\infty\int_0^\infty \mathcal{R}_2^{(a)}A_2(X - \tau_0)A_1(X - \tau_0 - \tau_1)A_1^*(X - 3\tau_0 - \tau_1)d\tau_0 d\tau_1 \\ &\quad + \int_0^\infty\int_0^\infty \mathcal{R}_2^{(b)}A_2(X - \tau_0 - \tau_1)A_1(X - \tau_0)A_1^*(X - 3\tau_0 - 2\tau_1)d\tau_0 d\tau_1, \end{aligned} \tag{3.7}$$

where the kernels $\mathcal{R}$ are given in Appendix A. The form of these jumps is somewhat different to that in the resonant triads (Mallier, 1996), where A_2 did not enter into the jump in D_{11}, which is somewhat fortuitous

because such a term would have necessarily been a quadratic of the form $A_1^* A_2$, and if such a jump had existed it would have precluded using the scaling considered here. In the present study, there are three additional cubic terms in the jump in D_{11} involving $A_1 A_2 A_2^*$ which were not present in Mallier (1996) because of the scaling used there. In the jump in D_{22}, we no longer have the quartic term in A_1, but there is an additional cubic term present here involving $A_2 A_2 A_2^*$ which was not present for the resonant triads. We note that the nonlinear kernel for the cubic term $A_1 A_1 A_1^*$ in the jump in D_{11} is the same as the kernel for the term $A_2 A_2 A_2^*$ in the jump in D_{22} (although of course the constants multiplying these terms are different); this kernel is simply that found by Goldstein and Choi (1989) in their study of a pair of interacting oblique waves.

If we pose a similar expansion near the critical layer at $y = -y_c$, we arrive at identical expressions for the jumps in the $D_{mn(-)}$ across the critical layer. Again, this is in contrast to the situation for the resonant triads where a number of the jumps cancelled as their signs were changed, and this is because of the different structure of the terms here.

4. Amplitude equations

Matching the expressions for the jumps obtained from both the outer expansion (2.9),(2.10) and the inner expansions (3.7), we arrive at our amplitude equations,

$$
\begin{aligned}
(4.1)\quad & \gamma^{(1a)} A_1 + \gamma^{(1b)} A_1' \\
&= -\frac{k_1}{2c_1} \int_0^\infty \int_0^\infty \mathcal{R}_1^{(a)} A_1^*(X - 2\tau_0 - \tau_1) A_1(X - \tau_0 - \tau_1) A_1(X - \tau_0) d\tau_0 d\tau_1 \\
&\quad - \frac{1}{2c_1} \int_0^\infty \int_0^\infty \mathcal{R}_1^{(b)} A_2^*(X - 3\tau_0 - \tau_1) A_2(X - 2\tau_0 - \tau_1) A_1(X - 2\tau_0) d\tau_0 d\tau_1 \\
&\quad - \frac{1}{2c_1} \int_0^\infty \int_0^\infty \mathcal{R}_1^{(c)} A_2^*(X - \tau_0 - 2\tau_1) A_2(X - \tau_1) A_1(X - 2\tau_0 - 2\tau_1) d\tau_0 d\tau_1 \\
&\quad - \frac{1}{2c_1} \int_0^\infty \int_0^\infty \mathcal{R}_1^{(d)} A_2^*(X - 3\tau_0 - 2\tau_1) A_2(X - \tau_1 - 2\tau_0) A_1(X - 2\tau_0 - 2\tau_1) d\tau_0 d\tau_1
\end{aligned}
$$

and

$$
\begin{aligned}
(4.2)\quad & \gamma^{(2a)} A_2 + \gamma^{(2b)} A_2' \\
&= -\frac{k_2}{4c_1} \int_0^\infty \int_0^\infty \mathcal{R}_1^{(a)} A_2^*(X - 2\tau_0 - \tau_1) A_2(X - \tau_0 - \tau_1) A_2(X - \tau_0) d\tau_0 d\tau_1 \\
&\quad - \frac{1}{4c_1} \int_0^\infty \int_0^\infty \mathcal{R}_2^{(a)} A_2(X - \tau_0) A_1(X - \tau_0 - \tau_1) A_1^*(X - 3\tau_0 - \tau_1) d\tau_0 d\tau_1 \\
&\quad - \frac{1}{4c_1} \int_0^\infty \int_0^\infty \mathcal{R}_2^{(b)} A_2(X - \tau_0 - \tau_1) A_1(X - \tau_0) A_1^*(X - 3\tau_0 - 2\tau_1) d\tau_0 d\tau_1 .
\end{aligned}
$$

A few remarks should be made about the form of these equations. Firstly, the equation for each mode involves a linear term, a cubic interaction with itself and a cubic interaction with the other mode. The kernel of the self-interaction cubic term is in both cases simply (a constant times) the kernel from Goldstein and Choi (1989), where the problem of a single pair of waves incident on a shear layer was studied, and because of this if only the varicose mode were present (that is $A_2 \equiv 0$), then the equation for A_1 reduces to that found by Goldstein and Choi (1989), as does that for A_2 if only the sinuous mode were present. Secondly, the cubic interaction between the two modes in the second equation (4.2) is of course precisely that found in the study of the resonant triads, but that in the first equation (4.1) is new. Due to the scaling used in the resonant triads, the only interaction

between the two oblique waves which could have entered into the corresponding equation would have been quadratic, *i.e.* of the form $A_1^* A_2$, but no such term was present, which is fortuitous from the point of view of the present study as such a term would have meant the scaling presented here was not possible. The coupling of these two equations is very interesting because for the resonant triads (Mallier, 1996), the varicose modes affected the development of the sinuous modes but not vice versa, whereas in the present problem, each mode affects the development of the other. This is in part because a different scaling was used for the resonant triads. As with similar equations of this form, the solutions A_1 and A_2 will become singular at some finite distance downstream, with the structure of the singularity being the same as that found in Goldstein and Choi, namely

$$A_1 \sim b_1/(X_s - X)^{5/2+i\psi}$$
$$A_2 \sim b_2/(X_s - X)^{5/2+i\tilde{\psi}}, \tag{4.3}$$

where ψ and $\tilde{\psi}$ are real (so the real parts of the exponent are the same for the two modes but the imaginary parts will differ) and b_1 and b_2 are complex. This singularity would be manifested in a real flow as extremely rapid growth, marking the onset of a subsequent more nonlinear stage governed by the complete Euler equations. It is interesting to note that if one mode were much smaller than the other, the equation for the larger wave would revert to that of Goldstein and Choi while the equation for the smaller wave would remain nonlinear, although the cubic self-interaction term would drop out, with the nonlinearity composed entirely of a cubic interaction between the two waves. For example, presumably in an unforced flow, the varicose mode would be very much smaller than the sinuous mode, then since the equation for A_1 would still involve nonlinear terms in A_2, the singularity would still arise in that equation and the varicose modes would still experience this very rapid growth, which in this case would be super-exponential, even though they were much smaller. This can be seem by replacing A_1 by νA_1 (with $\nu \ll 1$) in the amplitude equations and neglecting higher order terms in ν.

In *figures 1–4*, we present typical numerical solutions of the amplitude equations, plotting the $\log_{10}$ of the modulus of the (complex) amplitudes, $\log_{10} \mid A_1 \mid$ and $\log_{10} \mid A_2 \mid$. The numerical scheme used was similar to that employed by Goldstein and Choi (1989). The integrals in (4.1) and (4.2) were truncated to integrals over a finite interval and evaluated using a Newton-Coates formula and the tails of the integrals were estimated analytically using the behaviour of the amplitudes as $X \to -\infty$. A tenth-order Runge-Kutta scheme was used for for the numerical integration, and the computation was carried out on a Cray J90SE. The computation was started at some initial point X_0 during the linear growth phase (when the amplitudes are sufficiently small that that nonlinear terms can be neglected), where it is known that

$$A_1 \sim a_1 e^{\sigma_1 X}$$
$$A_2 \sim a_2 e^{\sigma_2 X}, \tag{4.4}$$

where the σ_i are the linear growth rates. The a_i are complex constants, but since it can be shown analytically that the solution to (4.1,4.2) is independent of the arguments of the a_i, it was assumed that they were real for the computations. The initial conditions were prescribed by specifying the angle θ and the values of the a_i. For all of the runs shown, we took $X_0 = -300$.

We present results corresponding to four different values of θ, the angle at which the pairs of waves are inclined to the plane of the jet. In *figures 1–4*, we present results for $\theta = \pi/8$, $\pi/6$, $\pi/4$ and $\pi/3$ respectively. We also consider the effect of varying the relative initial amplitudes of the waves. For each value of θ, we present two runs: run (a) with $a_1 = a_2 = 1$ and run (b) with $a_2 = 1$ again but with $a_1 = 10^{-4}$. It should be noted that in run (a), even though we set $a_1 = a_2$, the amplitudes of the two waves will differ in the linear regime because they have different linear growth rates. It can be seen that, as discussed earlier, the amplitudes

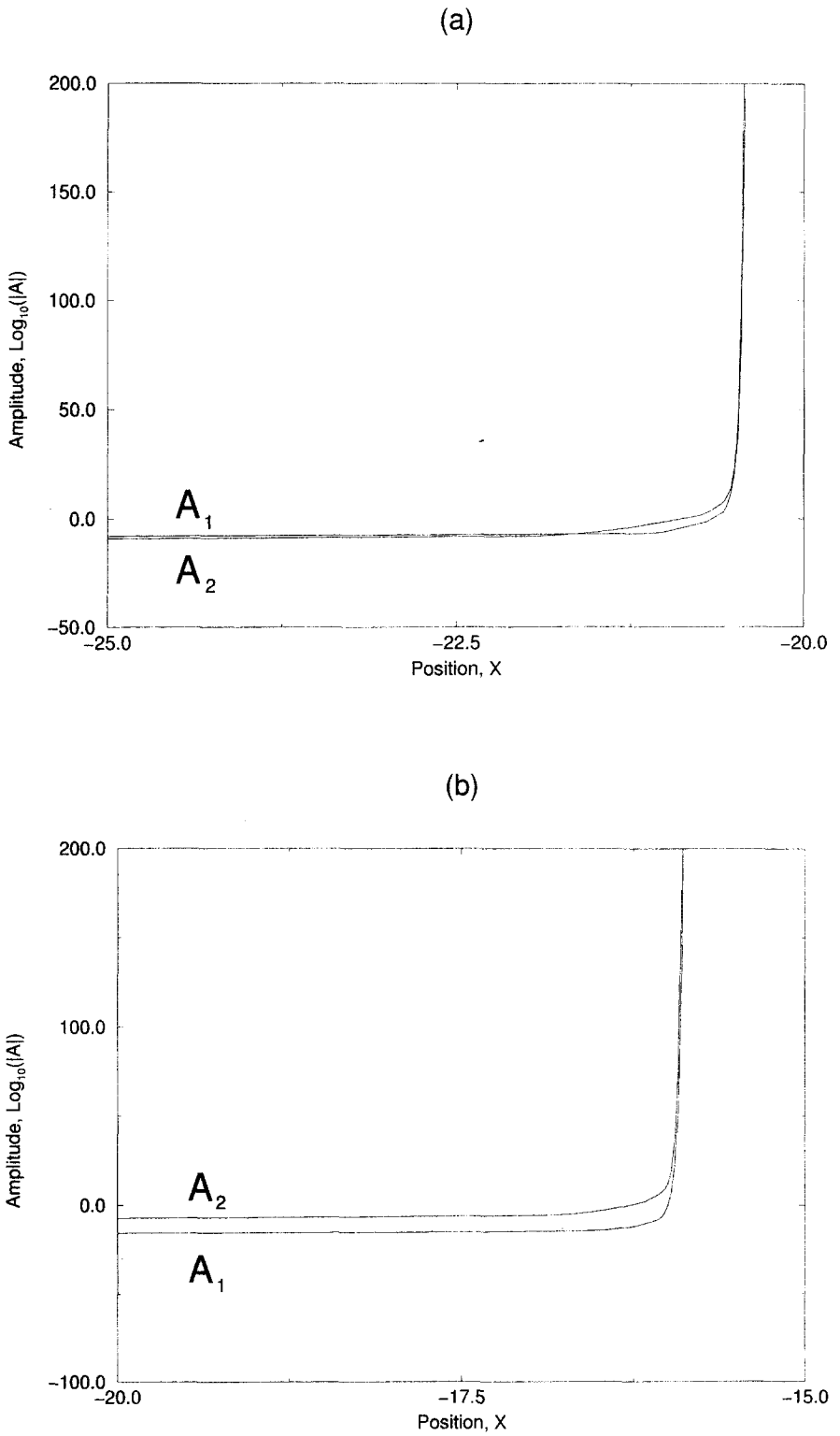

Fig. 1. – Evolution of the log of the modulus of the amplitudes, $\log_{10} \mid A_1 \mid$ and $\log_{10} \mid A_2 \mid$ for $\theta = \pi/8$. Initial conditions specified by (4.4) with $a_2 = 1$: (a) $a_1 = 1$; (b) $a_1 = 10^{-4}$.

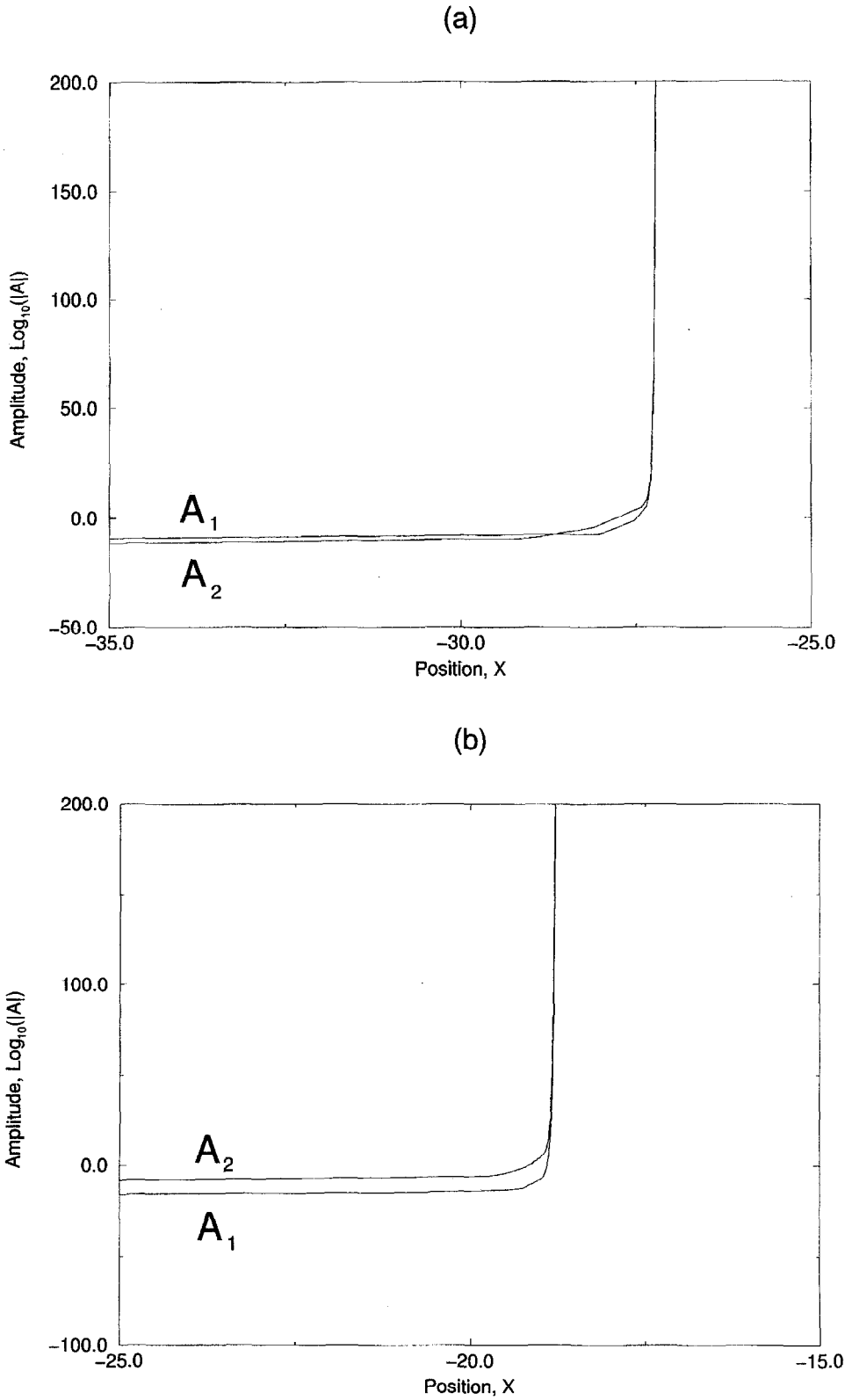

Fig. 2. – As in *Figure 1* but with $\theta = \pi/6$.

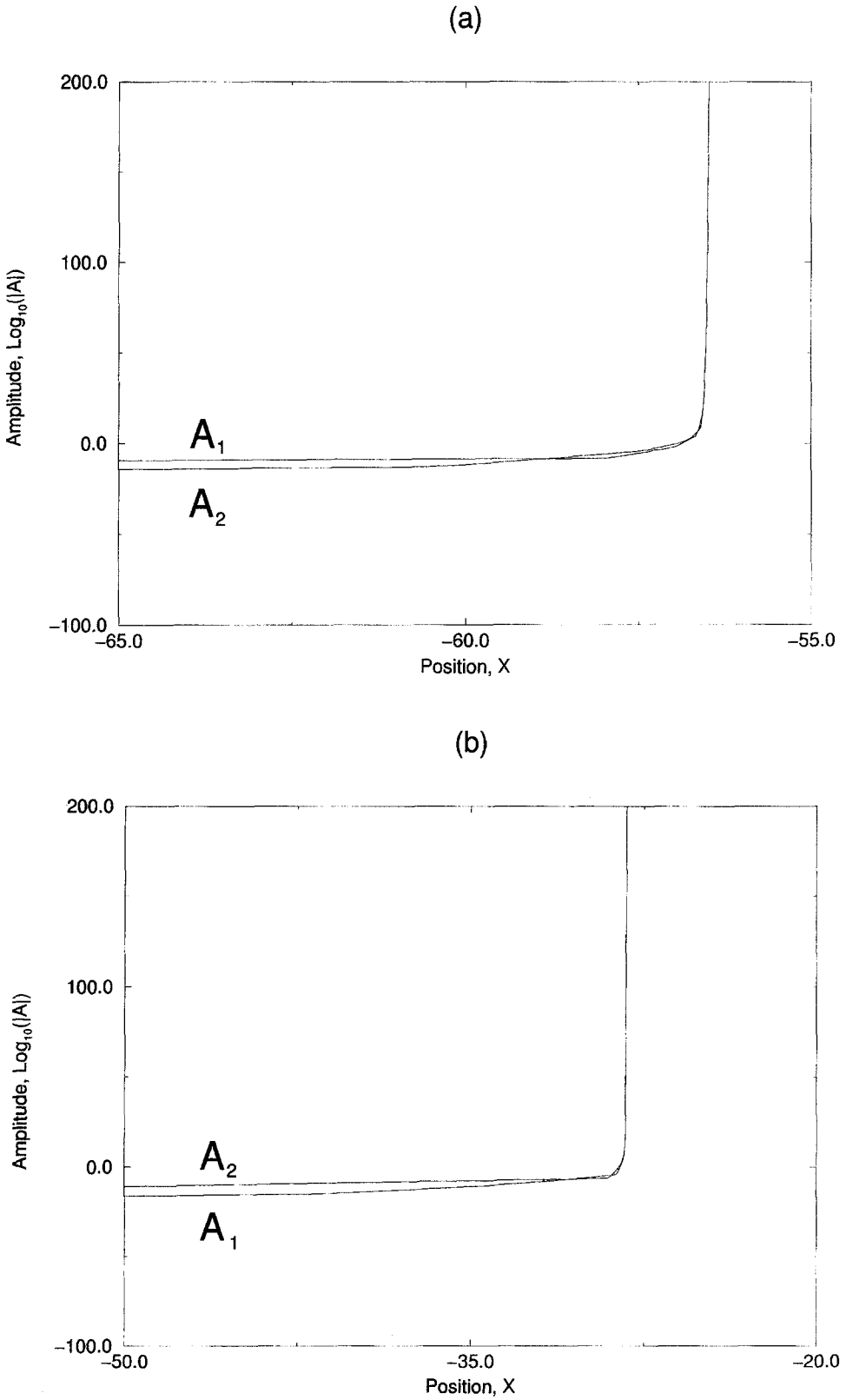

Fig. 3. – As in *Figure 1* but with $\theta = \pi/4$.

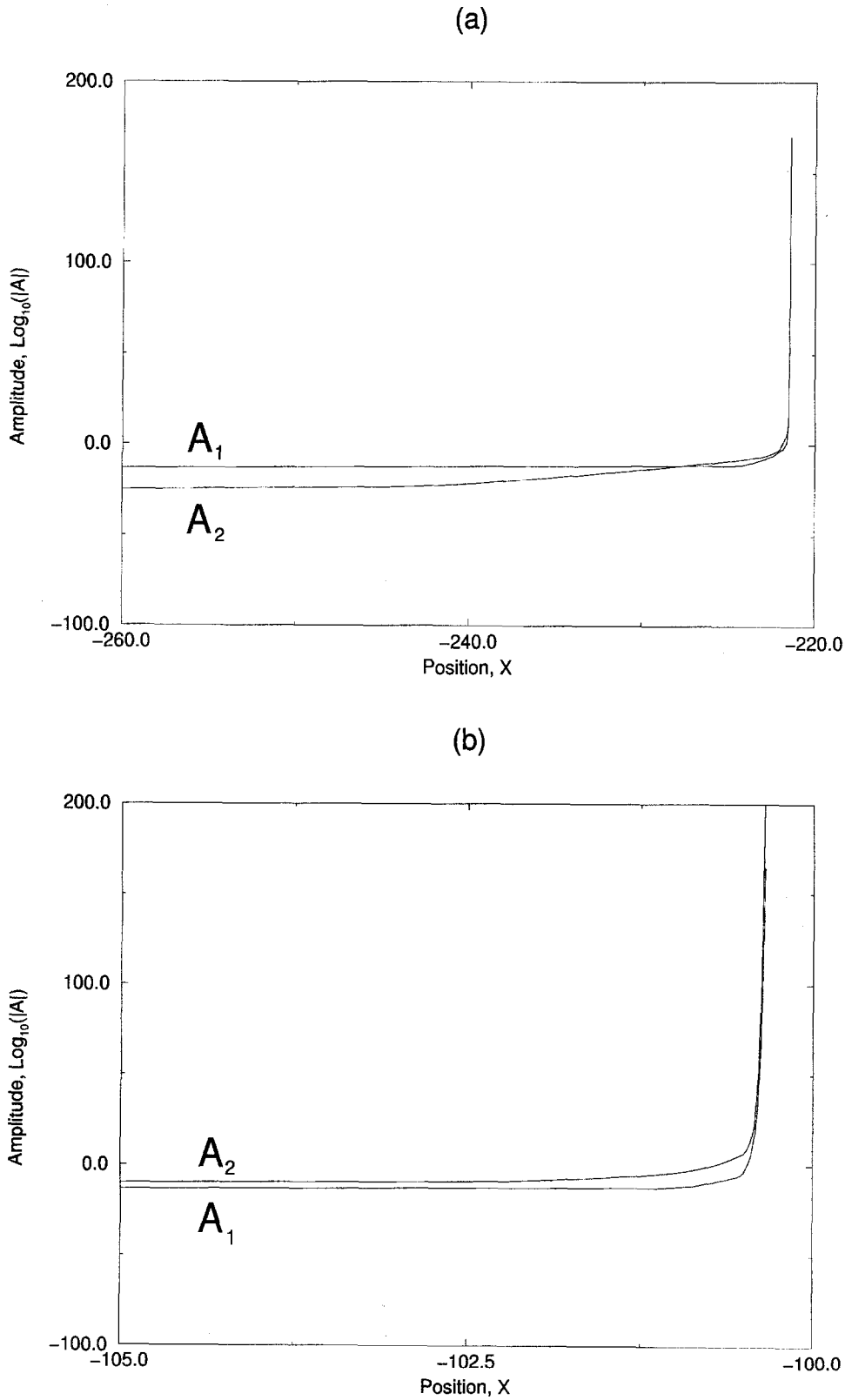

Fig. 4. – As in *Figure 1* but with $\theta = \pi/3$.

are initially very small and at first grow linearly in line with (4.4), with nonlinear effects becoming important further downstream. We found that A_2 began to exhibit nonlinear growth earlier that A_1 in all of the cases we examined except *figure 3b*, and that this nonlinear growth in A_2 was quickly coupled to A_1. The reason that *figure 3b* is special is that when $\theta = \pi/4$, the nonlinear self-interaction terms in (4.1) and (4.2) vanish, so that the nonlinear terms in the equation for A_1 are all of the form $\mid A_2 \mid^2 A_1$ while those in the equation for A_2 are of the form $\mid A_1 \mid^2 A_2$. Because of this, when $\theta = \pi/4$, the smaller mode will be affected the most by the nonlinear terms, and this is evident in *figure 3b*.

In each case we studied, the nonlinear growth led rapidly to a singularity in both amplitudes, with both modes having a singularity at the same location. In most of the cases studied, the two modes had comparable amplitudes immediately prior to the singularity, but in several (*figures 1b, 2b,4b*), A_2 was considerably larger than A_1 just before the singularity.

We also found that variations in both the angle θ or the ratio of the initial amplitudes may play a strong role in determining the location of the downstream singularity X_s. For example, decreasing a_1 while holding θ and a_2 fixed leads to a later onset of the singularity. This can be seen in *figure 1* where $\theta = \pi/8$. In *figure 1a*, we see that with $a_1 = a_2 = 1$, the growth first becomes nonlinear at roughly $X = -22$, leading to the singularity at $X_s = -20.5$. In *figure 1b*, with $a_2 = 1$ and $a_1 = 10^{-4}$, we see that the growth becomes nonlinear a little earlier, at about $X = -16.8$, leading to a singularity at $X_s = -15.8$.

For the cases we examined, it appears that increasing θ while holding the a_i fixed led to an earlier onset of the singularity. For example, in *figure 2*, with $\theta = \pi/6$, we see in *figure 2a* that when $a_1 = a_2 = 1$, the singularity occurs at about $X_s = -27.2$, which is much earlier than in the corresponding run with $\theta = \pi/8$ (*figure 1a*), and similarly, in *figure 2b*, with $a_2 = 1$ and $a_1 = 10^{-4}$, the singularity occurs at around $X_s = -18.7$, which is earlier than in *figure 1b*. The effect of further increasing the angle is illustrated in *figures 3* and *4*.

Finally in this section, we make some remarks on the effects of viscosity. It appears likely that viscous effects would modify this singular behavior slightly but it appears that at high Reynolds numbers the result is still meaningful, as evidenced by recent work by Wu (1995) and Lee (1997). Wu showed that viscosity delays the occurrence of the finite distance singularity but does not appear to be able to eliminate it. Since a full discussion of the effects of viscosity is beyond the scope of this article, the interested reader is referred to the studies by Wu and Lee for more details.

5. Concluding remarks

In the preceding sections, coupled amplitude equations (4.1) and (4.2) were derived governing the interaction of two pairs of oblique waves superimposed upon the Bickley jet, with one pair associated with either of the varicose and sinuous modes. The two pairs were assumed to be inclined at the same angle (θ) to the plane of the jet and their amplitudes were nominally of the same order of magnitude. Numerical solutions to the amplitude equations are presented in *figures 1–4*. The equations describe two successive stages of the evolution process: the initial linear growth stage for small disturbances, when the nonlinear terms in the evolution equations vanish, and a fully nonlinear stage, and that can be seen in the numerical solutions. Almost always, nonlinear effects became apparent in the sinuous waves first, with the varicose modes exhibiting nonlinear growth soon afterwards. For each case examined numerically, this nonlinear stage culminated in a singularity at a finite distance downstream, with both modes becoming singular at a finite distance downstream. The situation here appears somewhat different to that for the resonant triads, where the development of the varicose modes was affected by the sinuous modes but not vice versa. In the present study, where we have two pairs of oblique waves, the equations have a somewhat different coupling and the modes affect each other via the cubic nonlinearities in the amplitude equations.

It is also interesting to note that if one of the modes were much smaller than the other, then the equation for the dominant mode is simply that given by Goldstein and Choi (1989). One particular scenario that could be envisaged therefore is one where both modes are growing linearly, but with the sinuous mode dominant, as predicted by linear theory. When the nonlinear stage presented here is reached, the sinuous mode would experience very rapid growth and the singularity after a finite distance, and this singularity would be coupled back to the varicose modes which would also experience very rapid growth. This is a possible explanation for the asymmetry which has been observed to arise in some experiments on three-dimensional wakes (e.g. Corke *et al.*, 1992). This particular scenario was not possible with the resonant triads, where there was a parametric resonance stage during which the oblique varicose modes underwent very rapid (superexponential) growth but the other modes continued to grow linearly, leading to a stage in which the varicose modes dominated. Thus, there would appear to be a number of situations in which the present theory would appear to be more applicable than that presented in Mallier (1996), or for that matter in Wu (1996).

As mentioned in Section 1, one of the features of the Bickley jet is that the neutral varicose mode is the subharmonic of the neutral sinuous mode. However, what is required for the mechanism discussed in this study to be present is not that one of the neutral modes be the subharmonic of the other but rather that one of the *instability waves* be the subharmonic of the other (and even then a small amount of detuning would be permitted). Because of this, this mechanism should be present in other jet and wake flows which have two neutral modes.

Finally, we note that in a sense it is unfortunate that, at the moment, the theoretical investigations of nonlinear critical layers are ahead of the experimental investigations. As noted in section 1, some experimental evidence of the growth mechanisms for oblique disturbances to shear layers discussed here and elsewhere has been found (e.g. Corke and Kusek, 1993), but a lot more work remains to be done to clarify exactly when each mechanism is appropriate: in particular, the present work, and earlier studies, have demonstrated that there exist a number of interesting situations in the Bickley jet which have yet to be fully investigated experimentally or via numerical simulations.

Appendix A. Details of the analysis

The kernels for Section 3 are given by

$$\mathcal{R}_1^{(a)} = \tau_0\big(\tau_0(2\tau_0+\tau_1)+2\tau_1(\tau_0+\tau_1)\sin^2\theta\big)$$

$$\mathcal{R}_1^{(b)} = -\frac{2^7}{3^{5/2}}\cos^3\theta\sin^2\theta\tau_0\left(\tau_0^2-\frac{2}{3}\sin^2\theta\big(3\tau_0^2+2\tau_0\tau_1+\tau_1^2\big)\right)$$

$$\mathcal{R}_1^{(c)} = -\frac{2^4}{3^{5/2}}\cos^3\theta\sin^2\theta\tau_0\big(\tau_1(\tau_1-\tau_0)+4\sin^2\theta\tau_0(\tau_0+2\tau_1)-4\sin^4\theta\big(\tau_1^2-\tau_1^2\big)\big)$$

$$\mathcal{R}_1^{(d)} = -\frac{2^6}{3^{5/2}}\cos^3\theta\sin^2\theta(2\tau_0+\tau_1)(\tau_0+\tau_1)\big(\big(3-2\sin^2\theta\big)(\tau_0-\tau_1)-12\sin^4\theta\tau_1\big)$$

$$\mathcal{R}_2^{(a)} = -\frac{2^8\pi\sin^2\theta\cos^3\theta}{3^{5/2}}\tau_0^3$$

$$\mathcal{R}_2^{(b)} = \frac{2^7\pi\cos^3\theta\sin^2\theta}{3^{5/2}}\tau_0\big((2\tau_0+\tau_1)(7\tau_0+2\tau_1)-8\sin^2\theta\tau_0(3\tau_0+2\tau_1)-8\sin^4\theta\tau_1(\tau_0+\tau_1)\big).$$

The constants for Section 3 and Section 4 are given by

$$k_1 = -\frac{2^3\pi \sin^2\theta \cos^3\theta \cos 2\theta}{3^{5/2}}$$

$$k_2 = -\frac{2^{15/2}\pi \sin^2\theta \cos^3\theta \cos 2\theta}{3^{5/2}}$$

$$\gamma^{(1a)} = 1 - \frac{2y_c}{\sqrt{3}} + \frac{\imath\pi}{\sqrt{3}}$$

$$\gamma^{(1b)} = \frac{8\imath y_c}{3\sqrt{3}\cos\theta} - \frac{2\imath}{3\cos\theta} + \frac{\imath\cos\theta}{3} + \frac{2\pi}{3\sqrt{3}\cos\theta}$$

$$\gamma^{(2a)} = 2 + \frac{2y_c}{\sqrt{3}} - \frac{\imath\pi}{\sqrt{3}}$$

$$\gamma^{(2b)} = \frac{2\imath}{3\cos\theta} + \frac{2\imath\cos\theta}{3} + \frac{2\imath y_c}{3\sqrt{3}\cos\theta} - \frac{\pi}{3\sqrt{3}\cos\theta}.$$

Appendix B. Amplitude equations for the resonant triads

The amplitude equations derived in Mallier (1996) for the resonant triad case were of the form

$$\gamma^{(11a)}A_{11} + \gamma^{(11b)}A_{11}' = \int_0^\infty \mathcal{S}_{11}^{(a)} A_{20}(X-\tau_0)A_{11}^*(X-2\tau_0)d\tau_0 + \int_0^\infty\int_0^\infty \mathcal{S}_{11}^{(b)} A_{11}^*(X-2\tau_0-\tau_1)A_{11}(X-\tau_0-\tau_1)A_{11}(X-\tau_0)d\tau_0 d\tau_1$$

and

$$\gamma^{(20a)}A_{20} + \gamma^{(20b)}A_{20}' = \int_0^\infty\int_0^\infty\int_0^\infty \mathcal{S}_{20}^{(a)} A_{11}^*(X-3\tau_0-2\tau_1-\tau_2)A_{11}(X-\tau_0-\tau_1-\tau_2) \times A_{11}(X-\tau_0-\tau_1)A_{11}(X-\tau_0)d\tau_0 d\tau_1 d\tau_2 + \int_0^\infty\int_0^\infty \mathcal{S}_{20}^{(b)} A_{11}^*(X-3\tau_0-2\tau_1)A_{20}(X-\tau_0-\tau_1)A_{11}(X-\tau_0)d\tau_0 d\tau_1 + \int_0^\infty\int_0^\infty \mathcal{S}_{20}^{(c)} A_{11}^*(X-3\tau_0-\tau_1)A_{11}(X-\tau_0-\tau_1)A_{20}(X-\tau_0)d\tau_0 d\tau_1$$

and

$$\gamma^{(22a)}A_{22} + \gamma^{(22b)}A_{22}' = \int_0^\infty\int_0^\infty \mathcal{S}_{22}^{(a)} A_{11}^*(X-3\tau_0-\tau_1)A_{11}(X-\tau_0-\tau_1)A_{22}(X-\tau_0)d\tau_0 d\tau_1 + \int_0^\infty\int_0^\infty \mathcal{S}_{22}^{(b)} A_{11}^*(X-3\tau_0-2\tau_1)A_{22}(X-\tau_0-\tau_1)A_{11}(X-\tau_0)d\tau_0 d\tau_1 + \int_0^\infty\int_0^\infty \mathcal{S}_{22}^{(c)} A_{11}^*(X-3\tau_0-2\tau_1)A_{40}(X-\tau_0-\tau_1)A_{11}^*(X-\tau_0-2\tau_1)d\tau_0 d\tau_1 + \int_0^\infty\int_0^\infty \mathcal{S}_{22}^{(d)} A_{11}^*(X-3\tau_0-4\tau_1)A_{40}(X-\tau_0-\tau_1)A_{11}^*(X-\tau_0)d\tau_0 d\tau_1$$

and

$$\gamma^{(40a)}A_{40} + \gamma^{(40b)}A_{40}' = \int_0^\infty\int_0^\infty \mathcal{S}_{40}^{(a)} A_{11}^*(X-5\tau_0-4\tau_1)A_{40}(X-\tau_0-\tau_1)A_{11}(X-\tau_0)d\tau_0 d\tau_1 + \int_0^\infty\int_0^\infty \mathcal{S}_{40}^{(b)} A_{11}^*(X-5\tau_0-\tau_1)A_{11}(X-\tau_0-\tau_1)A_{40}(X-\tau_0)d\tau_0 d\tau_1,$$

where the kernels S were simple polynomials, and A_{11} and A_{20} represented the varicose oblique and plane waves respectively and A_{22} and A_{40} represented the sinuous oblique and plane waves. In deriving these equations, it was assumed that the oblique varicose waves (inclined at $\pm 60°$) had amplitudes of magnitude $\mathcal{O}(\varepsilon)$, while the oblique sinuous waves (also inclined at $\pm 60°$) and the plane varicose and sinuous waves all had amplitudes $\mathcal{O}\left(\varepsilon^{4/3}\right)$.

REFERENCES

CORKE T.C., KRULL J.D. and GHASSEMI M., 1992, Three-dimensional resonance in far wakes, *J. Fluid Mech.*, **239**, 99–132.

CORKE T.C., KUSEK S.M., 1993, Resonance in axisymmetric jets with controlled helical mode input, *J. Fluid Mech.*, **249**, 307–336.

GOLDSTEIN M.E., 1994, Nonlinear interaction between oblique waves on nearly planar shear flows, *Phys. Fluids A*, **6**, 42–65.

GOLDSTEIN M.E., CHOI S.W., 1989, Nonlinear evolution of interacting oblique waves on two-dimensional shear layers, *J. Fluid Mech.*, **207**, 97–120. Corrigendum, 1990, *J. Fluid Mech.*, **216**, 659–663.

GOLDSTEIN M.E., LEE S.S., 1992, Fully coupled resonant-triad interaction in an adverse-pressure-gradient boundary layer, *J. Fluid Mech.*, **245**, 523–551.

HICKERNELL F.J., 1984, Time-dependent critical layers in shear flows on the beta-plane, *J. Fluid Mech.*, **142**, 431–449.

KELLY R.E., 1968, On the resonant interaction of neutral disturbances in two inviscid shear flows, *J. Fluid Mech.*, **31**, 789–799.

LEE S.S., 1997, Generalized critical-layer analysis of fully coupled resonant-triad interactions in a free shear layer, *J. Fluid Mech.*, **347**, 71–103.

LEIB S.J., GOLDSTEIN M.E., 1989, Nonlinear interaction between the sinuous and varicose instability modes in a plane wake, *Phys. Fluids A*, **1**, 513–521.

MALLIER R., 1996, Fully coupled resonant triad interactions in a Bickley jet, *Eur. J. Mech., B/Fluids*, **15**, 507–526.

MALLIER R., MASLOWE S.A., 1994a, Parametric resonant triad interactions in a free shear layer, *Canadian Applied Mathematics Quarterly*, **2**, 91–113.

MALLIER R., MASLOWE S.A., 1994b, Fully coupled resonant triad interactions in a free shear layer, *J. Fluid Mech.*, **278**, 101–121.

SATO H., 1970, An experimental study of nonlinear interaction of velocity fluctuations in the transition region of a two-dimensional wake, *J. Fluid Mech.*, **44**, 741–765.

SATO H., SAITO H., 1978, Artificial control of laminar-turbulent transition of a two-dimensional wake by external sound, *J. Fluid Mech.*, **67**, 539–559.

SONDERGAARD R., MANSOUR N.N., CANTWELL B.J., 1994, The effect of initial conditions on the development of temporally evolving planar three dimensional incompressible wakes, *AGARD Conference Proceedings*, **AGARD–CP–551**.

SONDERGAARD R., CANTWELL B.J., MANSOUR N.N., 1997, Direct numerical simulation of a temporally incompressible plane wake: effect of initial conditions on evolution and topology, *Joint Institute for Aeronautics and Acoustics Technical Report*, **JIAA TR 118**.

WILLIAMSON C.H.K., PRASAD A., 1993a, A new mechanism for oblique wave resonance in the 'natural' far wake, *J. Fluid Mech.*, **256**, 269–313.

WILLIAMSON C.H.K., PRASAD A., 1993b, Acoustic forcing of oblique wave resonance in the far wake, *J. Fluid Mech.*, **256**, 313–341.

WU X., 1992, The nonlinear evolution of high-frequency resonant-triad waves in an oscillatory Stokes layer at high Reynolds number, *J. Fluid Mech.*, **245**, 553–597.

WU X., 1995, Viscous effects on fully coupled resonant-triad interactions: an analytical approach, *J. Fluid Mech.*, **292**, 377–407.

WU X., 1996, On an active resonant triad of mixed modes in symmetric shear flows: a plane wake as a paradigm, *J. Fluid Mech.*, **317**, 337–368.

WU X., LEE S.S., COWLEY S.J., 1993, On the weakly nonlinear three-dimensional instability of shear layers to pairs of oblique waves: The Stokes layer as a paradigm, *J. Fluid Mech.*, **253**, 681–721.

WU X., STEWART P.A., 1996, Interaction of phase-locked modes: a new mechanism for the rapid growth of three-dimensional disturbances, *J. Fluid Mech.*, **316**, 335–372.

WYGNANSKI I., CHAMPAGNE F., MARASLI B, 1986, On the large scale structures in two dimensional, small deficit turbulent wakes, *J. Fluid Mech.*, **168**, 31–71.

(Received 24 April 1997;
revised 1 July 1998;
accepted 28 September 1998.)